Application of the Multilayer Analysis to Contaminant Transport along Porous Media Flow with Variable Coefficients and two-input Sources

Thomas Tjock-Mbaga[1]✉* | **Ali Zarma**[2] | **Patrice Ele Abiama**[1,3] | **Jean-Marie Ema'a Ema'a** [4] | **Germain Hubert Ben-Bolie**[1]

1. Laboratory of Nuclear Physics, Department of Physics, Faculty of Science, University of Yaounde I, P.O. Box 812, Cameroon
2. Department of physics, University of Maroua, P.O. Box 814, Maroua Cameroon
3. Nuclear Technology Section, Energy Research Laboratory, Institute of Geological and Mining Research, Yaounde, Cameroon
4. Higher Teacher Training College, Department of physics, University of Bertoua, P.O. Box 652, Cameroon.

Article Info	ABSTRACT
Article type: Research Article **Article history:** Received: 26.06.2022 Revised: 10.09.2022 Accepted: 22.10.2022 **Keywords:** Advection-dispersion Multilayer model Laplace transform Two sources Finite domain	This study presents a new approach to solve the one-dimensional solute transport equation with variable coefficients and two input sources in a finite porous media. The medium is divided into m-layers porous media with constant averages coefficients in each transport problem. The transport equations in layer i-1 and i are coupled by imposing the continuity of solute concentration and the dispersive flux at the interfaces of the layers. Unknown functions representing the dispersive flux at the interfaces between adjacent layers are introduced allowing the multilayer problem to be solved separately on each layer in the Laplace domain before being numerical inverted back to the time domain. The obtained solution was compared with the Generalized Integral Transform Technique (GITT) and numerical solutions for some problems of solute transport with variables coefficients in porous medium present in the literature. The results show a good agreement between both solutions for each of the studied problem. An example of application considering an advective-dispersive transport problem with a sinusoidal time-dependent emitting rate at the boundary was study in order to illustrate the effect of sinusoidal frequency on solute concentration.

INTRODUCTION

Human activities and industrialization have considerably increased the numbers of pollutant sources in water, soil, air and specially in groundwater. Many of them are subject of studies due to their importance or the damage they can cause to living organisms. Hence there is a need to provide fast contaminant remediation and quality monitoring of the groundwater system. The transport of a solute in porous media is traditionally modeled by the advection-dispersion equation (ADE). The ADE can be solved numerically or analytically. Analytical solutions are still pursued by many scientists because they are relatively transparent with respect to model inputs and outputs, and they can provide better physical insights into the problems (Park & Zhan, 2001).

*Corresponding Author Email: *ttjockmbaga@yahoo.fr*

Analytical solutions of ADE with variable coefficients in semi-infinite porous media abound recent years in the literature (Kumar et al., 2010; Jaiswal et al., 2011; Djordjevich & Savovic, 2013; Singh et al., 2015; Sanskrityay et al., 2016; Das et al., 2017; Sanskrityay et al., 2018; Yadav & Kumar, 2018; Thakur et al., 2019; Chaudhary et al., 2020; Chaudhary & Sink, 2020). The solutions are obtained using change of variables and techniques such as the Laplace transform, Green function method. Alternatively, literature contains several analytical solutions of ADEs in finite porous media with constants or variables coefficients. Liu et al. (2000) presented how to implement the GITT to solve the one-dimensional (1-D) ADE in heterogeneous porous media with source/sink term, coupled with either linear or nonlinear sorption and decay. The GITT coupled with the LTT were used by Chen & Liu (2011) to solve analytically a 1-D ADE in a finite spatial domain with an arbitrary time-dependent inlet boundary condition. For a finite spatial domain, the 1-D ADE considering the sorption and desorption of solute, with arbitrary space dependent coefficients was solved analytically using the GITT (Skaggs et al., 2007). Pérez Guerrero et al. (2009) presented a new analytical method to solve a 3-D ADE in a finite domain with time varying boundary condition for both transient and steady-state regimes using change of variables in combination with the Classic Integral Transform technique (CITT). Pérez Guerrero & Skaggs (2010) presented a general analytical solution for linear 1-D solute transport in heterogeneous porous media. They employed the integrating factor to obtain a transport equation that has a self-adjoint differential operator, and the solution was found using the GITT. Chen et al. (2011) presented an analytical solution of two-dimensional ADE in cylindrical coordinates using a combination of the second kind finite transform method and the GITT. Recently, Bharati et al. (2017); Bharati et al. (2018) and Bharati et al. (2019) presented an analytical solution of solute transport with distance depending coefficients without source term using the GITT with a new regular Sturm-Liuville problem (SLP) with a self-adjoint operator to derive analytical solutions in a finite domain. Although the studies proposed novel approaches to solve the ADE, they have some limitations and difficulties to be applied in complex problems.

Analytical solutions for layer media are not left out on the literature. The LLT was used by Al-Niami & Rushton (1979) to obtain analytical solutions of solute transport in finite layered media with constant boundary conditions. Leij et al. (1991) also applied the Laplace transform to derive an analytical solution to the 1-D ADE (without decay term) on a semi-infinite two-layer medium with continuity of concentration and dispersive flux at the interfaces between adjacent layers. Moreover, Leij & van Genuchten (1995) used the LTT to obtain an approximate analytical solution to the 1-D ADE in semi-infinite two-layer medium. In each layer, solute concentration in the Laplace domain was approximated by an infinite series before the analytical inversion. Later Liu et al. (1998) used the GITT to solve a 1-D multi-layer for conservative solute transport problem in finite media with arbitrary time-varying inlet concentration. Their analytical solution was found to be easily applied for an arbitrary number of layers. A few years later Pérez Guerrero et al. (2013) used the method of Liu et al. (1998) to obtain analytical solution of ADE for a non-conservative solute transport with constant inlet boundary. One of the difficulties encountered when applying the integral transform to this type of problem is the determination of the eigen-functions and the resolution of the transcendental equation.

To overcome the difficulties encountered when solving multilayer problem using the GITT, some authors have had the idea of reutilizing the Laplace transform while introducing unknown functions at each interface. The consequence of this approach is the transformation of the multi-layer problem into several isolated layer problems which can be solve easily with the help of Laplace transform. Among these recent works, we can cite (Carr & Turner, 2016; Rodrigo & Worthy, 2016; Zimmerman et al., 2016; Carr, 2020; Carr, 2021).

The aim of this study is to extend the work of Carr (2020) to solve the 1-D ADE of conservative and reactive solute with space and time dependent coefficients and two inputs localized at the boundaries of the domain. More precisely, we intend to show that the multilayer model can

reproduce the concentration profiles for this type of problems whatever the expressions of the coefficients in the ADE and the forms of the boundary and initial conditions. This will allow in the future to solve the ADE problems in a finite porous media with variables coefficients without many difficulties like those related to the transcendental equation. To our knowledge, no other study in the literature has ever been conducted on this issue. This approach is all the more innovative in that it circumvents the difficulties encountered when using conventional approaches and also overcomes their limitations.

MATERIALS AND METHODS

In this paper, we consider a 1-D pollutant transport problem in space and time dependent transport velocity and dispersion coefficient in heterogeneous structure. The mathematical formulation of the ADE for solute transport in 1-D flow under linear equilibrium sorption can be written in general form as:

$$R(x)\frac{\partial C}{\partial t} = \frac{\partial}{\partial x}\left[D(x,t)\frac{\partial C}{\partial x} - v(x,t)C \right] - \mu(x)C + \gamma(x,t) \qquad (1)$$

which describes processes of advection, dispersion, equilibrium sorption, and decay. In Eq. (1), $R(x)$ is the linear retardation factor, $C(x,t)$ $[ML^{-3}]$ is the aqueous solute concentration of the dispersing pollutant mass at a position $x[L]$ of the medium and at a time $t[T]$, $\mu(x)$ is the first order decay rate per volume of aqueous solution under linear sorption $[T^{-1}]$, the non-homogeneous term $\gamma(x,t)$ represents an arbitrary space and time variable zero-order production. The left-hand side of Eq. (1) represents change in solute concentration in liquid with time in linear equilibrium sorption. The right-hand side of the Eq. (1) represents the influence of the dispersion on the solute concentration distribution by the first term and the change of the solute concentration due to advective solute transport by the second term. The third term of the right-hand represents the first-order decay of solute in the medium. The fifth term represent the zero-order production ($\gamma(x,t) > 0$) or sink ($\gamma(x,t) < 0$) for solute which represents internal/external production or sink of the solute in the medium.

Two phenomena are responsible to solute spreading, the mechanical dispersion and the diffusion. Generally, both $D(x,t)$ and $v(x,t)$ are assumed to be functions of space and time. The expression of each parameter depends on the properties of the geological formation. For study, many theories are used for the spatio-temporal dependence of the velocity and dispersion coefficient (e.g. Scheidegger 1957; Rumer 1962; Freeze & Cherry 1979). The velocity and dispersion coefficient are expressed by single function on space and time-dependent as follow:

$$v(x,t) = v_0 h_2(x)\varphi_2(pt) \quad D(x,t) = \left(D_0 + D^*\tau \right) h_1(x)\varphi_1(pt) \qquad (2)$$

where τ is the tortuosity, $D_0[L^2T^{-1}]$, $D^*[L^2T^{-1}]$ and $v_0[LT^{-1}]$ are respectively constant mechanical dispersion coefficient, molecular diffusion coefficient and velocity in a steady flow domain through a homogeneous porous medium. $h_1(x)$ and $h_2(x)$ are the non-dimensional space dependent functions for velocity and dispersion, respectively. $p[T^{-1}]$ is a coefficient whose dimension is inverse of the time variable, it represents the unsteady parameter. The unsteady functions $\varphi_1(pt)$ and $\varphi_2(pt)$ are expressions in non-dimensional variable (pt). $P=0$ corresponds to the temporally independent parameters. Generally, the expressions of unsteady functions are chosen such that $\varphi_j(pt) = 0$ for $p = 0$ or $t = 0$. The former case represents the steady flow and the latter case represents the initial state.

The source/sink is also expressed by single function on space and time-dependent as that

proposed by Chen et al. (2017) and Kumar et al., (2019):

$$\gamma(x,t) = \gamma_0 P(x)q(t) \tag{3}$$

where γ_0 is the uniform zero-first order production coefficient $[ML^{-3}T^{-1}]$.
Using Eqs. (2) and (3) in Eq. (1) leads to the following transport equation:

$$R(x)\frac{\partial C}{\partial t} = \frac{\partial}{\partial x}\left[D_{x_0}h_1(x)\varphi_1(pt)\frac{\partial C}{\partial x} - v_0 h_2(x)\varphi_2(pt)C\right] - \mu(x)C + \gamma_0 P(x)q(t) \tag{4}$$

The formulation of our problem to be complete by assuming a set of initial and boundary conditions. Initially, the porous medium is supposed to contain a background pollutant concentration with arbitrary distribution which can be expressed as a linear combination of some input contaminant concentration in liquid phase and solid phase, respectively. The initial concentration may be written in general form as:

$$C(0,t) = f_l(x) + f_s(x) = f(x) \tag{5}$$

In this study, we consider the solute transport to be affected at the two ends of the domain (two pollutants sources). A general robin boundary condition with flexible input source distribution are taken into consideration at the porous medium. Thus, boundary conditions are written in general form as follow:

$$a_0 C(0,t) - b_0 \frac{\partial C(0,t)}{\partial x} = g_0(t), \quad t \geq 0 \tag{6}$$

$$a_L C(L,t) - b_L \frac{\partial C(L,t)}{\partial x} = g_L(t), \quad t \geq 0 \tag{7}$$

where $L[L]$ is the length of the porous medium.
In the boundary conditions Equations (6) and (7), a_0, b_0, a_L and b_L are constants and $g_0(t)$ and $g_L(t)$ are arbitrary specified functions of time with the subscripts 0 and L denoting the inlet ($x = 0$) and outlet ($x = L$), respectively (Figure 1). It is important to note that b_0 and b_L must be both nonnegative, at least one of a_0 or b_0 must be nonzero and at least one of a_L and b_L must be nonzero.
The multi-layer analysis is performed in the advection-dispersion transport problem with variable parameters formulated in Eqs. (4)-(7). The solution method begins with transforming the transport problem with variable coefficients into m-transports problems with time dependent coefficients. For this aim, the porous medium is divided into m-layers porous media partitioned as $0 = x_0 < x_1 < x_2 < ... < x_{m-1} < x_m = L$ (Figure 1). The pollutant concentration in layer i is denoted by $C_i(x,t)$ ($i = 1,...,m$) where $x \in [x_{i-1}, x_i]$ represents the distance from the inlet at $x = 0$. The
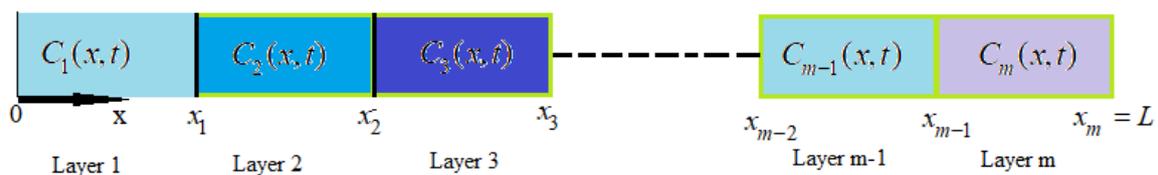
Fig. 1. Partitioning of heterogeneous medium into m-layers media with constant coefficents.

governing solute transport equation in Eq. (4) may be expressed in the ith-layer as:

$$R_i \frac{\partial C_i}{\partial t} = D_i \varphi_1(pt) \frac{\partial^2 C_i}{\partial x^2} - v_i \varphi_2(pt) \frac{\partial C_i}{\partial x} - \mu_i C_i + \gamma_i q(t), \quad x_{i-1} \leq x \leq x_i \qquad (8)$$

where the coefficients $D_i[L^2 T^{-1}]$, $v_i[L T^{-1}]$, $\mu_i[T^{-1}]$ and $\gamma_i[ML^{-3}T^{-1}]$ are the constant average value of coefficient for in the layer i (Moreira et al., 2006; Moreira et al., 2009; Moreira et al., 2010; Ema'a Ema'a et al., 2015), defined in general form by:

$$\eta_i = \frac{1}{x_i - x_{i-1}} \int_{x_{i-1}}^{x_i} \eta(x) dx \qquad (9)$$

The solute transport Eqs. (8) are subject to the following initial and boundary conditions in each layer:

$$C_i(x,0) = f_i; \quad x_{i-1} \leq x \leq x_i \qquad (10)$$

$$a_0 C_1(0,t) - b_0 \frac{\partial C_1(0,t)}{\partial x} = g_0(t), \quad t \geq 0 \qquad (11)$$

$$a_L C_m(0,t) - b_L \frac{\partial C_m(0,t)}{\partial x} = g_L(t), \quad t \geq 0 \qquad (12)$$

where $f_i = \frac{1}{x_i - x_{i-1}} \int_{x_{i-1}}^{x_i} f(x) dx$

In order to relate the concentration of layer i to that of layer i+1, we assume the continuity of the concentration and dispersive flux at the interfaces between adjacent layers:

$$C_i(x_i,t) = C_{i+1}(x_i,t) \qquad (13)$$

$$\theta_i D_i \frac{\partial C_i}{\partial x}(x_i,t) = \theta_{i+1} D_{i+1} \frac{\partial C_{i+1}}{\partial x}(x_i,t) \qquad (14)$$

Let us introduce a new space and time variables, X and T, respectively, defined as Kumar et al. (2011):

$$X = \int \frac{\varphi_2(pt)}{\varphi_1(pt)} dx = \frac{\varphi_2(pt)}{\varphi_1(pt)} x \qquad (15)$$

$$T = \int \frac{\varphi_2^2(pt)}{\varphi_1(pt)} dt \qquad (16)$$

Since $\varphi_1(pt)$ and $\varphi_2(pt)$ are dimensionless functions, T as the same dimension of that of

time variable t. Moreover, the selection criteria for $\varphi_j(pt)$ verify that $T = 0$ at $t = 0$. So the nature of the initial condition does not change in the new time domain. The advection-diffusion problem in Eq. (8) reduces to one with constant coefficients which is:

$$R_i \frac{\partial C_i}{\partial T} = D_i \frac{\partial^2 C_i}{\partial X^2} - v_i \frac{\partial C_i}{\partial X} - k_i C_i + \gamma_i(T) \quad l_{i-1} \le X \le l_i \tag{17}$$

where $k_i = \mu_i \dfrac{\varphi_2^2(pt)}{\varphi_1(pt)}$

The conditions in Eqs. (11) - (15) may be written in terms of new independent variables as:

$$C_i(X, 0) = f_i; \quad l_{i-1} \le X \le l_i \tag{18}$$

$$a_0 C_1(0, T) - b_0 \frac{\partial C_1(0, T)}{\partial X} = g_0(T), \quad T > 0 \tag{19}$$

$$a_L C_m(0, T) - b_L \frac{\partial C_m(0, T)}{\partial X} = g_L(T), \quad T > 0 \tag{20}$$

$$C_i(l_i, T) = C_{i+1}(l_i, T) \tag{21}$$

$$\theta_i D_i \frac{\partial C_i}{\partial X}(l_i, T) = \theta_{i+1} D_{i+1} \frac{\partial C_{i+1}}{\partial X}(l_i, T) \tag{22}$$

Following the generalized semi-analytical method for solving multilayer transport model proposed by Carr (2020) as detailed in Appendix A, the pollutant concentration in layer i in the Laplace domain can be expressed as:

$$\overline{C}_1(X, s) = A_1(X, s)G_0(s) + B_1(X, s)G_1(s) + P_1(X, s), \tag{23}$$

$$\overline{C}_i(X, s) = A_i(X, s)G_{i-1}(s) + B_i(X, s)G_i(s) + P_i(X, s), \quad i = 2, ..., m-1 \tag{24}$$

$$\overline{C}_m(X, s) = A_m(X, s)G_{m-1}(s) + B_m(X, s)G_L(s) + P_m(X, s) \tag{25}$$

where the functions $P_i(X, s)$, $A_i(X, s)$ and $B_i(X, s)$ ($i = 1, ..., m$) are defined in Table 1 of Carr (2020).

The determination of unknow interface functions $G_i(s)$ ($i = 1, ..., m-1$) becomes possible by imposing continuity of concentration in the Laplace domain ($\overline{C}_i(X, s)$) in each interface layers (Carr and Turner 2016; Rodrigo and Worthy 2016; Carr and March 2018, Carr 2020, Carr 2021):

$$\overline{C}_i(l_i, s) = \overline{C}_{i+1}(l_i, s) \tag{26}$$

Substituting Eqs. (23)–(25) into the system of Eqs. (26), the result is a linear system which

can be expressed in matrix form as:

$$\mathbf{Ay} = \mathbf{b} \tag{27}$$

where $\mathbf{y}$ is a column matrix with elements $G_i(s)$, elements of $(m-1) \times (m-1)$ tridiagonal matrix $\mathbf{A}$ ($\{a_{ij}\} \in \mathbb{C}^{(m-1) \times (m-1)}$) and $(m-1)$-length vector $\mathbf{b}$ ($b_i \in \mathbb{C}^{(m-1)}$) ($i = 1,...,m-1$), are given by:

$$a_{1,1} = B_1(l_1,s) - A_2(l_1,s),$$
$$a_{1,2} = -B_2(l_1,s),$$

$$a_{i,i-1} = A_i(l_i,s), \quad i = 2,...,m-2,$$

$$a_{i,i} = B_i(l_i,s) - A_{i+1}(l_i,s), \quad i = 2,...,m-2,$$

$$a_{i,i+1} = B_{i+1}(l_i,s), \quad i = 2,...,m-2,$$

$$a_{m-1,m-2} = A_{m-1}(l_{m-1},s),$$

$$a_{m-1,m-1} = B_{m-1}(l_{m-1},s) - A_m(l_{m-1},s),$$

$$b_1 = P_2(l_1,s) - P_1(l_1,s) - A_1(l_i,s)G_0(s),$$

$$b_i = P_{i+1}(l_i,s) - P_i(l_i,s), \quad i = 2,...,m-2,$$

$$b_{m-1} = P_m(l_{m-1},s) - P_{m-1}(l_{m-1},s) - B_m(l_{m-1},s)G_L(s),$$

The solution of solute concentration for $ith-layer$ ($C_i(X,T)$) in the time is obtain using the inversion Laplace transform $\overline{C}_i(X,s)$ given by:

$$C_i(X,T) = L^{-1}\left\{\overline{C}_i(X,s)\right\} = \frac{1}{2\pi i}\int_{\Gamma} e^{st}\,\overline{C}_i(X,s)ds \tag{28}$$

where Γ represents a Hankel contour that begins $-\infty - i0$, winds around the origin and terminates at $-\infty + i0$ (Trefethen et al. 2006). The integration of Equation (28) in the complex domain is obtained by introducing the complex variable $z = st$, and using residue calculus approach described by Trefethen (see Trefethen et al. (2006) for full details) to numerically invert the Laplace transform:

$$C_i(X,T) = L^{-1}\left\{\overline{C}_i(X,s)\right\} = -\frac{2}{T}R_e\left\{\sum_{k\in O_N} w_k\overline{C}_i(X,s_k)\right\} \tag{29}$$

where N is even, is the set of positive odd integers less than N, $s_k = z_k / t$ and w_k, $z_k \in \mathbb{C}$ are the residues and poles of the best (N, N) rational approximation to e^z on the negative real line. Both w_k and z_k are constants, which are independent of x and t and computed using a supplied MATLAB function (Trefethen et al. 2006, Fig 4.1).

RESULTS AND DISCUSSION
Validation of the multilayer model

We now demonstrate the capabilities of multilayer analysis to produce the correct results using tests cases problems selected in the literature. The input boundaries conditions in each end of the domain can be a robin type or a Dirichlet type. There for, four combinations of input boundary are considered. A MATLAB code implementing our semi-analytical solution and producing the results in this section is an adaptation of MATLAB code download from github.com/elliotcarr /Carr2020a.

● *Case 1: Dirichlet- Dirichlet (D-D) boundaries*

For this combination of input boundary, the following advection dispersion problem in groundwater reservoir with steady flow is considered:

$$R\frac{\partial C}{\partial t} = \frac{\partial}{\partial x}\left[D_{x_0}(1+ax)^n\frac{\partial C}{\partial x} - u_0(1+ax)C\right] - \mu C + \gamma_0\exp(-(x-\beta))\exp(-\lambda t) \tag{30}$$

obtained by setting $h_1(x) = (1+ax)^n$, $h_2(x) = (1+ax)$, $\varphi_1(pt) = \varphi_2(pt) = 1$, $q(t) = \exp(-\lambda t)$ and $p(x) = \exp(-(x-\beta))$.

The time-dependent linear equilibrium between the solute substance in the solid–liquid phase given by Sim & Chrysikopoulos (1996) and Singh & Das (2015) is considered for this problem:

$$S = Fk_dC \tag{31}$$

where F represents the mass fraction of sorption particles where sorption is instantaneous, K_d is referred to as the distribution coefficient $[L^3M^{-1}]$.

$R = \theta + \frac{FK_df\rho_b}{\eta}$ (Chaudhary et al., 2020) and $a[L^{-1}]$ represents the heterogeneity parameter, $S(x,t)$ $[ML^{-3}]$ is the solid phase concentration, θ is the volumetric water content, ρ_b is the bulk density of porous media $[ML^{-3}]$, η is the porosity of the porous media, $\mu = \mu_l + \mu_s\rho_bFk_d$ (μ_l and μ_s are the first order decay rate of the liquid an solid phases concentration respectively $[T^{-1}]$).

The expressions of groundwater velocity and the dispersion coefficient follow the dispersion theory according to which the dispersion is proportional to the nth-power of the space velocity ($D \propto u^n$) (Freeze & Cherry, 1979), where n is considered as 1.0, 1.5, and 2.0, respectively.

In this problem, if the solute distribution coefficient K_d is negligible (i.e. $K_d \approx 0$), the retardation factor R becomes equal to water content θ. Since water content (θ) is less than 1, so the retardation factor R becomes less than 1 for the case mentioned above, this indicates that only a fraction of liquid phase concentration participates in the transport mechanism.

For short special domain, Chaudhary et al. (2020) proposed to use $\exp(-\sec(\lambda x))$ as distribution of background concentration in the liquid phase because, its decreasing rate is much slower than exponential and could well represent slow movement of groundwater. Therefore, the following initial condition is considered:

$$C(0,t) = f(x) = C_l^0\exp(-\sinh(\lambda x)) + K_i^s \tag{32}$$

where $C_l^0[ML^{-3}]$ is the uniform solute distribution in the liquid phase and $K_i^s[ML^{-3}]$ is the solute distribution in the solid phase.

The input parameters values used are given by Singh & Kumari (2014), $C_l^0 = 0.01$ mg/L, $K_s^i = 0.01$ mg/L, $u_0 = 0.01$ $m/year$, $D_0 = 0.01$ $m^2/year$, $D^* = 0.002$ $m^2/year$, $f = 0.8$, $F = 0.5$ $K_d = 0.01$, $\mu_s = 0.13$ $/year$, $\mu_l = 0.0027$ $/year$, $a = 0.5$ $/m$. $\beta = 3$ m and the

uniform source term $q_0 = 0.02 \; mg \, / \, L \; year$. The gravel and sandstone geological formations are considered here with average porosity η and bulk density   as follows (Manger, 1963; Freeze & Cherry, 1979) : $\eta = 0.3$ (sandstone), 0.5 (gravel) ; $\rho_b = 2.49$ (sandstone), 2.68 (gravel).

The medium is divided into four layers and the constants average values are calculated for each coefficient with the formula in Eq. 10. The transport parameters in each layer, initial conditions and boundary conditions for each are provided in Tables 1 and 5.

Figures 2 and 3 illustrate the comparison of pollutant concentration for the multilayer

Table 1. Transport parameters, geometry and initial conditions for problem 1.

L [m]	i	x_i [m]	n	D_i [m^2 / year]	u_i [m / year]	γ_i [m / Lyear]	θ_i [$-$]	f_i [mg / L]
	1		1	0.00224	0.0112	0.02332	0.4	0.0036788
	2			0.00264	0.0132	0.01813	0.4	0.0036788
	3			0.00296	0.0148	0.014841	0.4	0.0036789
	4			0.00336	0.0168	0.01158	0.4	0.0036789
	1	0.3	1.5	0.002374	0.0112	0.02332	0.4	0.0036788
	2	0.5		0.003034	0.0132	0.01813	0.4	0.0036788
	3	0.7		0.003602	0.0148	0.014841	0.4	0.0036789
	4	1		0.004358	0.0168	0.01158	0.4	0.0036789
1	1		2	0.002518	0.0112	0.02332	0.4	0.0036788
	2			0.003489	0.0132	0.01813	0.4	0.0036788
	3			0.004385	0.0148	0.014841	0.4	0.0036789
	4			0.005654	0.0168	0.01158	0.4	0.0036789

Table 2. Transport parameters, geometry and initial conditions for problem 2.

L [km]	i	x_i [km]	$Pe = 0.845$		$Pe = 1.833$		R_i	γ_i	θ_i [$-$]	μ_i [day^{-1}]	f_i [mg / ml]
			D_i [km^2 / year]	u_i [km / year]	D_i [km^2 / year]	u_i [km / year]					
	1	0.1	0.720685	0.6060	0.6060	0.71710	1	0	0.4	0	0
	2	0.25	0.747619	0.6210	0.6210	0.73485	1	0	0.4	0	0
1	3	0.5	0.791408	0.6450	0.6450	0.76325	1	0	0.4	0	0
	4	0.75	0.8472546	0.6750	0.6750	0.79875	1	0	0.4	0	0
	5	0.9	0.892804	0.6990	0.6990	0.82715	1	0	0.4	0	0
	6	1	0.9216852	0.7140	0.7140	0.8449	1	0	0.4	0	0

Table 3. Transport parameters, geometry and initial conditions for problem 3.

L [m]	i	x_i [m]	m	D_i [m^2 / day]	u_i [m / day]	R_i	γ_i	θ_i [$-$]	μ_i [day^{-1}]	f_i [mg / ml]
	1	10		2.050	1.025	1	0.0	0.4	0.002	0
	2	20		2.150	1.075	1	0.0	0.4	0.002	0
60	3	30	6	2.250	1.125	1	0.0	0.4	0.002	0
	4	40		2.350	1.175	1	0.0	0.4	0.002	0
	5	50		2.450	1.225	1	0.0	0.4	0.002	0
	6	60		2.550	1.275	1	0.0	0.4	0.002	0

Table 4. Transport parameters, geometry and initial conditions for example of application.

L [m]	i	x_i [m]	m	D_i [m^2 / day]	u_i [m / day]	R_i	γ_i	θ_i [−]	μ_i [day^{-1}]	f_i [mg / ml]
	1	10		2.050	1.025	1	0.0	0.4	0.002	0
	2	20		2.150	1.075	1	0.0	0.4	0.002	0
60	3	30	6	2.250	1.125	1	0.0	0.4	0.002	0
	4	40		2.350	1.175	1	0.0	0.4	0.002	0
	5	50		2.450	1.225	1	0.0	0.4	0.002	0
	6	60		2.550	1.275	1	0.0	0.4	0.002	0

Table 5. Boundary values parameters for each problem.

Problems	a_0	b_0	a_L	b_L	$g_0(t)$	$g_L(t)$
1 **Dirichlet-Dirichlet**	1	0	1	0	$C_0 \exp(-0.002t)$	$0.5C_0 \exp(-0.002t)$
2 **Robin-Dirichlet**	v_1	D_1	1	0	C_0	$0.5C_0$
Dirichlet-Robin	1	0	v_m	D_m	C_0	$0.5C_0$
3 **Robin-Robin**	v_1	D_1	v_m	D_m	$C_a + C_b \exp(-t)$	$0.5[C_a + C_b \exp(-t)]$
Example of application	v_1	D_1	1	0	$C_0(1+\sin(\omega t))$	$0.25C_0(1+\sin(\omega t))$
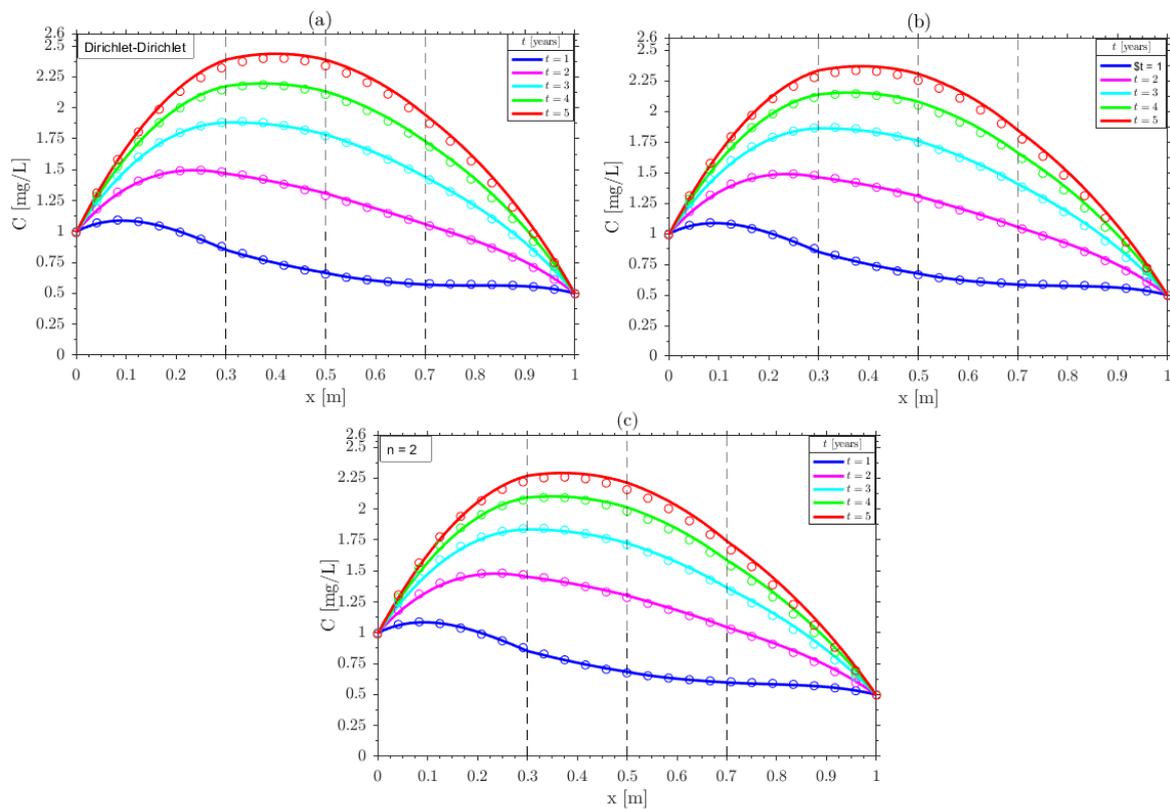
Fig. 2. Comparison of the multilayer solution and the GITT solution for problem 1, in sandstone geological formation, for different values of n.
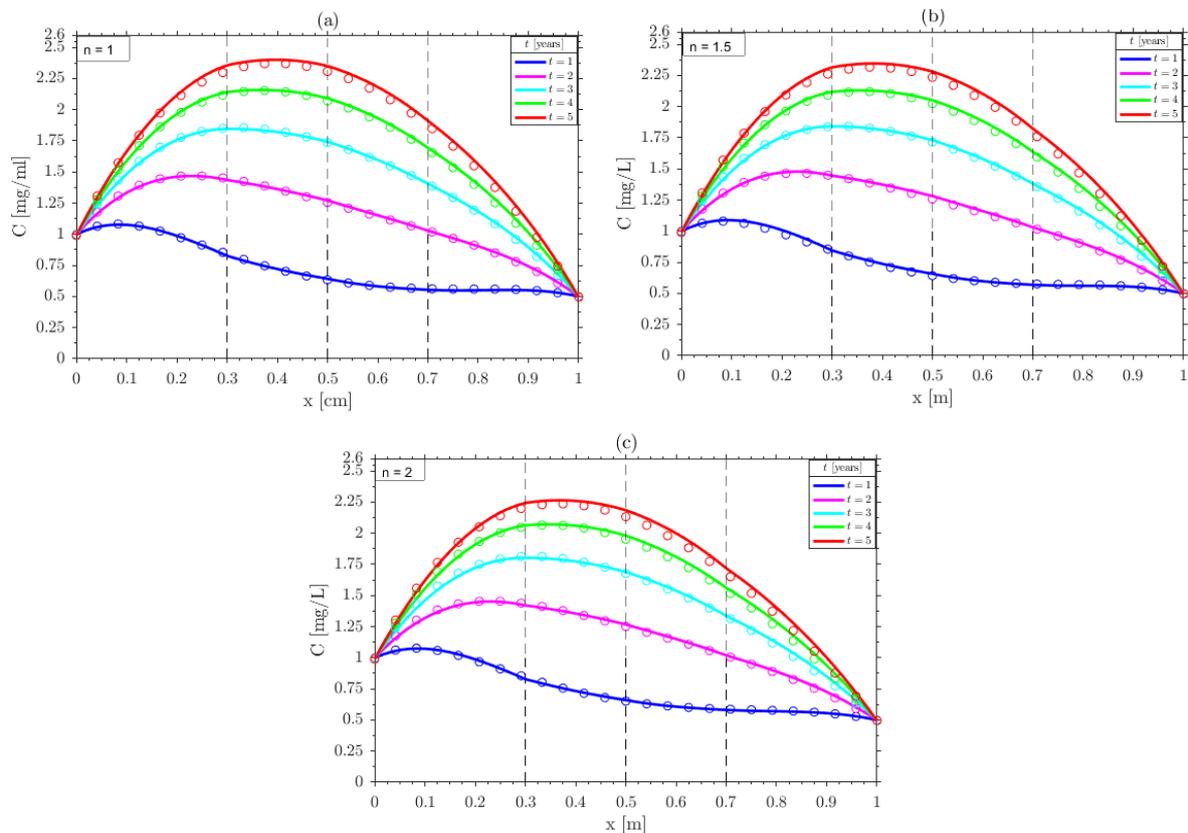
Fig. 3. Comparison of the multilayer solution and the GITT solution for problem 1, in gravel geological formation, for different values of n.

solution and the GITT solution (Bharati et al., 2017; 2018; 2019). The solids lines represent the concentration for the multilayer solution and the circles symbols represent the concentration for the GIIT solution. The curves show that, for each value of n and both geological formations, the solute concentration in the reservoir at each time increases with traveling distance from approximate value of 1.0 mg/L at $x = 0$ m to a maximum value of concentration, then decreases back to 0.5 mg/L at the end of the domain. This build-up of concentration is due to the concentration effect of the additional source term in the reservoir that decreases with distance. The solute build-up depends on the geological formation and on the value of n, for a fixed time. The distance concerned by the solute build-up is very important due to the presence of two contaminant sources, each acting separately at the boundary of the reservoir. The comparison between the multilayer solution and the GITT solution show that, both solutions are in good agreement as shown by the higher value of maximum error between both solutions in Table 6.

● *Case 2: Robin- Dirichlet (R-D) or Dirichlet-Robin (D-R) boundaries*

For this combination of inputs boundary, the following Problem of solute transport in groundwater with spatio-temporal dependent coefficients, without adsorption is considered:

$$\frac{\partial C}{\partial t} = \frac{\partial}{\partial x}\left[D_{x_0}(1+ax)^n \varphi(pt)\frac{\partial C}{\partial x} - u_0(1+ax)\varphi(pt)C \right] \tag{33}$$

Table 6. Maximum errors.

	Problem 1					
	Sandstone			Gravel		
	$n=1$	$n=1.5$	$n=2$	$n=1$	$n=1.5$	$n=2$
$t=1$ _year_	0.0038	0.0034	0.0028	0.0034	0.0032	0.0028
$t=2$ _years_	0.0074	0.0068	0.0075	0.0067	0.0067	0.0083
$t=3$ _years_	0.0119	0.0118	0.0125	0.0102	0.0108	0.0135
$t=4$ _years_	0.0184	0.0179	0.0196	0.0153	0.0167	0.0204
$t=5$ _years_	0.0342	0.0356	0.0364	0.0328	0.0352	0.0356

	Problem 2			
	(a)	**(b)**	**(c)**	**(d)**
$t=0.05$ _day_	0.008	0.0072	0.00302	0.0027
$t=0.1$ _day_	0.00557	0.00554	0.0067	0.00183
$t=0.15$ _day_	0.0083	0.0084	0.0083	0.00153
$t=0.25$ _day_	0.0112	0.0106	0.0076	0.00201
$t=0.5$ _day_	0.0124	0.0114	0.0054	0.00323

	Problem 3			
$t=0.5$ _day_	$t=1$ _day_	$t=2$ _days_	$t=3$ _days_	$t=4$ _days_
0.0023	0.0082	0.0056	0.0032	0.0033

corresponding to $h_1(x)=(1+ax)^n$, $h_2(x)=(1+ax)$, $\varphi_1(pt)=\varphi_2(pt)=\varphi(pt)=\exp(-0.01t)$ and $R=1$. The same problem was studied by Bharati et al. (2018) in case of steady flow. For those choice of unsteady functions, $X=x$ and $T=100(1-\exp(-0.01t))$.

This problem considers solute transport along porous media flow with spatial dispersivity in fractal & Euclidean framework. For the illustration, only the fractal framework of dispersivity is considered ($n=1.5$). Initially, the porous medium is considered solute free, the decay rate and zero order production are considered to be zero. We consider also two cases of problem studied by Bharati et al. (2018) concerning Peclet number greater than one and Peclet number less than one. Recall that the Peclet number is defined as follow $Pe=\frac{v_0 L}{D_0}$. For $Pe>1$, it represents advection dominated solute transport while for $Pe<1$ it represents dispersion dominated solute transport. The input parameters used for this problem are (Bharati, 2018): $a=0.2\ km^{-1}$, $v_0=0.6\ km/year$, $D_0=0.71\ km^2/year$ (for Peclet number less than 1) and $u_0=0.71\ km/year$, $D_0=0.6\ km^2/year$ (for Peclet number greater than 1).

The medium is divided into six layers and the constants average values are calculated for each coefficient with the formula in Eq. 10. The transport parameters for each layer are shown in Table 2 and the conditions in Table 5. Figure 4 (a, b, c and d) compares the multilayer solution obtained for six layer and the MATLAB solver *pdepe* numerical solution for the original problem, for Robin-Dirichlet boundaries (a, b) and Dirichlet-Robin boundaries (c, d), respectively. The curves are obtained for two values of the Peclet number representing the two descriptions of transport mentioned above. The common values for Figures (4.a) and (4.c) are $v_0=0.71\ km/year$ and $D_0=0.6\ km^2/year$ and for Figures (4.b) and (4.d) $u_0=0.6\ km/year$ and $D_0=0.71\ km^2/year$. The curves illustrate that for the Robin-Dirichlet boundaries,
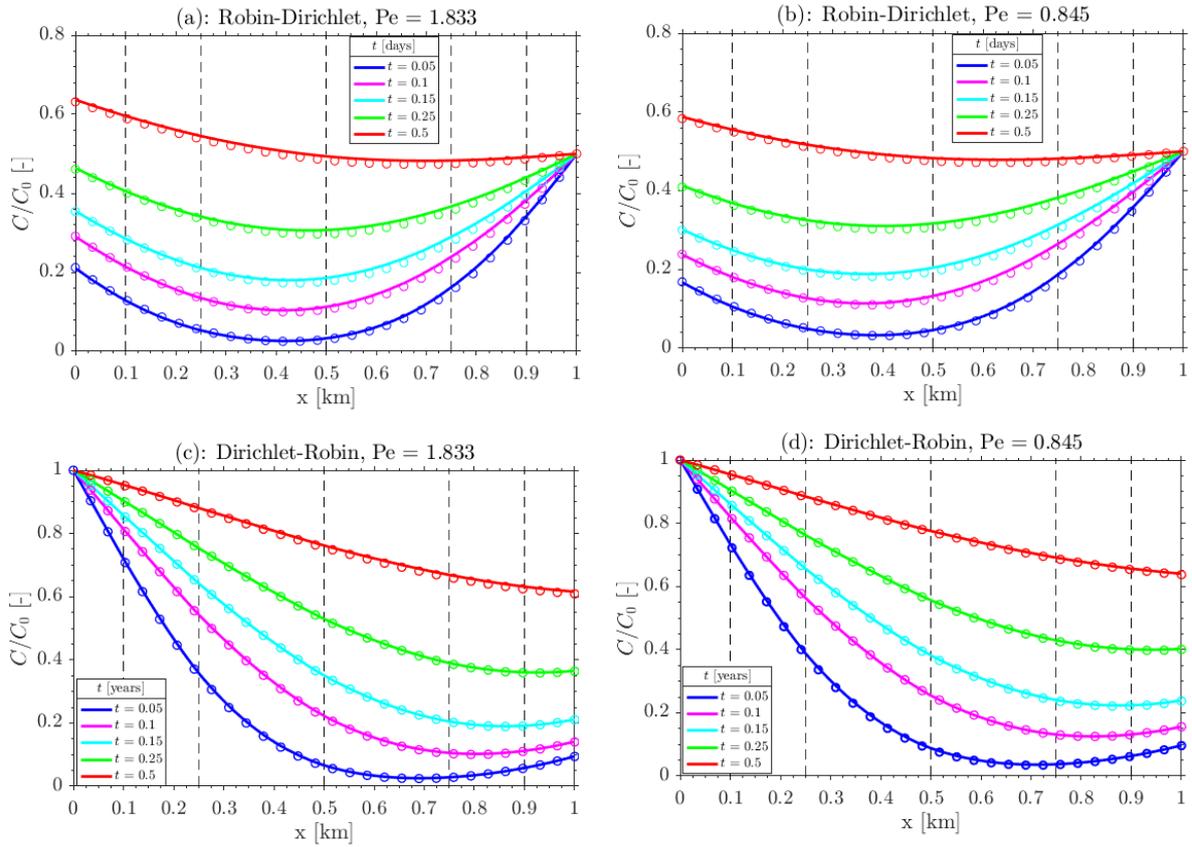
Fig. 4. Comparison of the multilayer solution and the GITT solution for Problem 2.

the solute concentration decreases slightly with traveling distance from a value imposed by the boundary condition at $x = 0$ m to a minimum value of concentration, then increases to 0.5 value at the end of the domain. While for the Dirichlet-Robin boundaries, the pollutant concentration decreases with traveling distance from a value of 1.0 at $x = 0$ m to a minimum value of concentration, then increases to a concentration value at the end of the domain given by the outlet input boundary. These pollutant concentration strengths in both boundaries combination is due to the presence of the two input sources localized at the boundaries of the domain. The curves also demonstrate that both solutions are in excellent agreement for each choice of the pairs of values u_0 and D_0, as shown by the higher value of maximum error between both solutions in Table 6. These results verify that the multilayer model reproduces well the original model in heterogeneous medium.

● *Case 3: Robin- Robin (R-R) boundaries*

In this case, we consider the following steady state flow transport problem with space variable dispersion coefficient, velocity, decay coefficient and retardation factor studied by Liu et al. (2000):

$$R(x)\frac{\partial C}{\partial t} = \frac{\partial}{\partial x}\left(D(x)\frac{\partial C}{\partial x} - v(x)C \right) - \mu(x)C + \gamma(x) \tag{34}$$

For this problem, the studied porous medium of length $L = 20$ cm has the following properties,
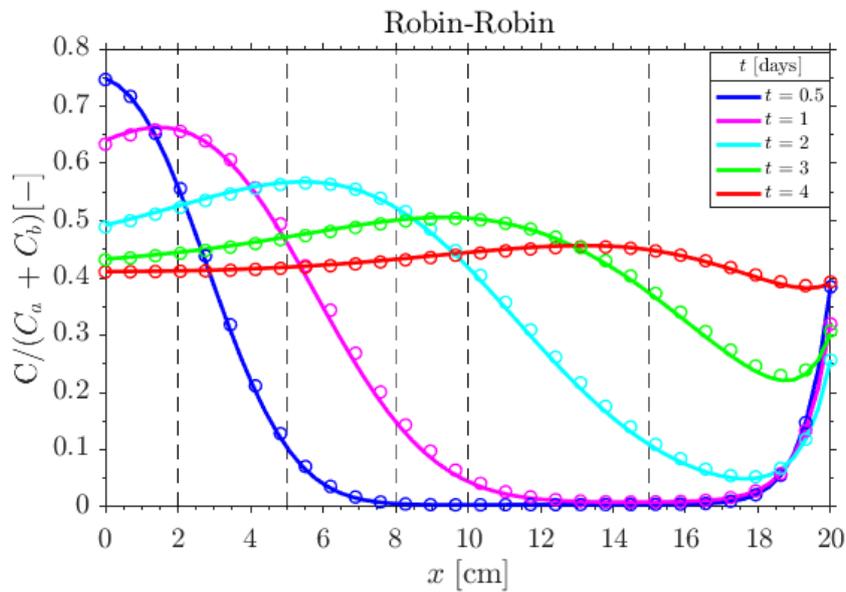
Fig. 5. Comparison of the multilayer solution and the GITT solution for Problem 3.
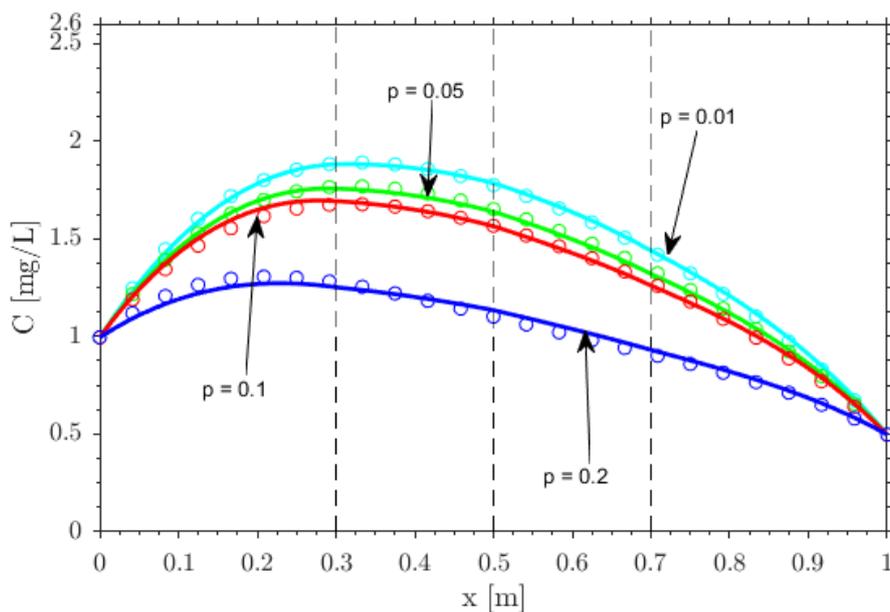
Fig. 6. Effect of unsteady parameter on solute concentration obtained with multilayer model.

$R(x) = 2.4 + 0.04x$, $v(x) = 14 - 0.2x \ cm/d$, $D(x) = 10 - 0.1x \ cm^2/d$, $\mu(x) = -(0.1 + 0.01x) \ day^{-1}$ and $\gamma(x) = 0.001x + 0.01$. A Robin type concentration with time variable input concentration are imposed at the boundaries ($g_{0,L}(t) = C_a^{0,L} + C_b^{0,L} 0.6 \exp(-t)$). The parameters $C_a^{0,L}$ and $C_b^{0,L}$ are chosen such that the input concentration must be equal to 1 at $t = 0$ at the inlet ($C_a^0 = 0.4$ and $C_b^0 = 0.6$) and 0.5 at the outlet ($C_a^L = 0.2$ and $C_b^L = 0.3$). A zero-initial pollutant concentration is assumed. The porous medium is divided into six layers, the parameters values obtained for each layer are shown in Table 3. The numerical solution using the MATLAB solver *pdepe* and the multilayer solution obtain six layers are compared in Fig. 5. It emerges for the curves that both solutions are in good agreement at all the time at all the positions. Thus, the multilayer is able

to reproduce the solute concentration in heterogeneous porous media for this type of problem.

As illustrated in Figs. (2) and (3), the accuracy of the multilayer model depends to the observed time in the case of time dependent production term. Now we investigate the effect of unsteady parameter to the multilayer model.

Fig. 6 illustrates the effect of unsteady parameter on solute concentration pattern in case 1 for a fractal dispersivity at $t = 3$ $years$. For the illustration, the gravel geological formation is considered. The concentrations are plotted for four values of unsteady parameter ($p = 0.01$, 0.05, 0.1 and 0.2 yr^{-1}). The figure elucidates that the concentration level at all the positions decreases with the increasing value of unsteady parameter for this type of time production function. We also observe that the accuracy of the multilayer model decreases with the increasing value of p. However, whatever the value of p, the RMSE remains in an acceptable zone such that the multilayer model can be used in the case of time dependent production term.

Example of application

An example of application that is rarely noted in the literature but haves many real world hydrological applications are discussed below. Special attention is paid to periodically time-dependent boundary at the source. This example considers an advective-dispersive transport problem with a sinusoidal time-dependent emitting rate at the boundary $g_{0,L}(t) = C_{0,L}(1 + \sin(\omega t))$. Where $\omega[T^{-1}]$ is the frequency of the sinusoidal boundary input. In this application we do not consider the zero-order production and initial distribution. Such example application can be used for the prediction of biochemical oxygen demand (BOD) concentration in groundwater with two input sources, resulting from waste leachate of periodical landfills discharge concentration. We consider a combination of Robin-Dirichlet boundaries. Also, we consider a medium in which the dispersion coefficient is proportional to the velocity ($n = 1$). The following transport parameters are used for this application example (Chen et al., 2017) $v_0 = 1$ m day^{-1}, $D_0 = 2$ $m^2 day^{-1}$, $a_1 = 1$, $a = 0.005$ m^-. The value of a is chosen such that the groundwater velocity remains less than 2 m day^{-1}, which is the highest value of groundwater velocity (Bharati, 2017). The medium is devised into six layers as shown in Table 4. Fig. 7.a and 7.b depicts the temporal evolution of the spatial concentration profiles for frequency of the sinusoidal periodic input function $\omega = 0.5$ and 0.25 day^{-1} respectively. For $\omega = 0.5$ day^{-1}, $g(t)$ has the maxima at $\omega t = 4k\pi - 3\pi$, inflection point (from positive to negative) at $\omega t = 4k\pi - 2\pi$, minima at $\omega t = 4k\pi - \pi$, and inflection point (from negative to positive) at $\omega t = 4k\pi$, respectively. While, for $\omega = 0.25$ day^{-1} $g(t)$ has the maxima at $\omega t = 8k\pi - 6\pi$, inflection point (from positive to negative) at $\omega t = 8k\pi - 4\pi$, minima at $\omega t = 8k\pi - 2\pi$, and inflection point (from negative to positive) at $\omega t = 8k\pi$, respectively. Figure 7.a clearly demonstrates that, the pollutant concentration exhibits four different strength corresponding to the four particulars points of the input function. Also, the periodic boundary input affects only the concentration profile near the inlet boundary. The periodic amplitudes of the concentration profile are quickly attenuated due to the heterogeneity of the medium causing a higher dispersion process which result is the mitigation of the concentration wave.

Figure 7.b illustrate the pollutant concentration distribution profiles at the same time used in Figure 7.a. The curves shown that for the time corresponding to the particular points on input function i.e. ($\omega t = 2\pi$, 4π, 6π and 8π), the concentration profiles are similar to those of Figure 7.a for corresponding times. But the pollutant concentration level at these times is higher for $\omega = 0.25$ day^{-1} in comparison to $\omega = 0.5$ day^{-1}. Each of the other time has its own pollute concentration distribution. However, the concentration wave mitigates far to the inlet boundary for $\omega = 0.25$ day^{-1} in comparison to $\omega = 0.5$ day^{-1}.

Figures 7.c and 7.d show the concentration breakthrough curves at different locations for $\omega = 0.5$ day^{-1} and $\omega = 0.25$ day^{-1} respectively. These curves clearly illustrate that for intermediate positions, the periodic time-dependent concentration wave only presents near
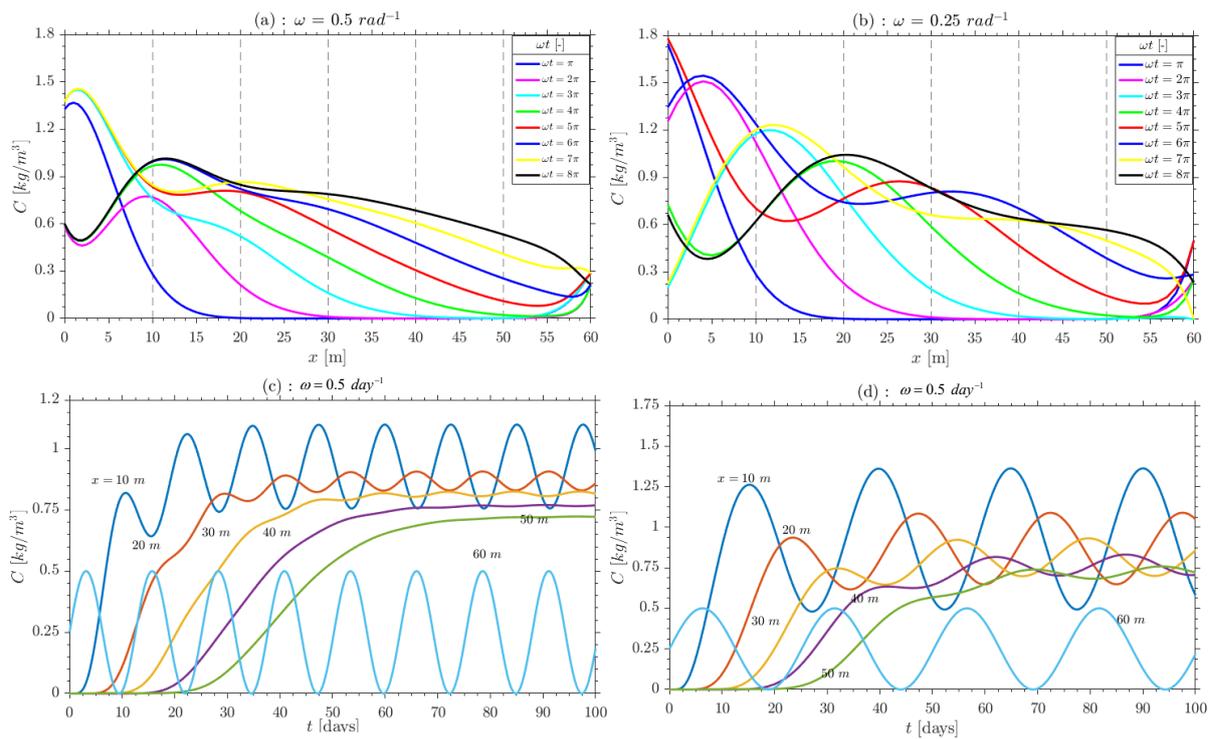
Fig. 7. Pollutant concentration trend (a) and (b) and breakthrough curves (c) and (d) for biochemical oxygen demand (BOD) concentration in groundwater with two input sources involving a sinusoidal time-dependent emitting rate.

the inlet boundary for $\omega = 0.5 \ day^{-1}$. While for $\omega = 0.25 \ day^{-1}$, the periodic time-dependent concentration wave presents in each of intermediate positions. However, at the far end of the domain ($x = 60 \ m$), the concentration for both values of ω presents the periodic time-dependent concentration wave given by the input function at this point. Over all, figures 7.c and 7.d also illustrate the amplitude of the periodic time dependent concentration is quickly attenuate in the case of $\omega = 0.5 \ day^{-1}$ than $\omega = 0.5 \ day^{-1}$.

In summarize, the frequency of the periodic boundary input at the inlet and the location influences the effect of the dispersion process on the propagation of the periodic concentration wave. But, the second input concentration at the outlet of the domain does not influence this process, it just influences the concentration pollutant level.

CONCLUSION

In this paper, the multilayer model was applied to solve a 1-D ADE with variable coefficients under general initial and boundary conditions. The ADE with variable coefficients is transformed into a set of m-equations with time dependent coefficients, coupled by the continuity of the concentration and the flux in the interfaces of layer adjacent. After introducing novel space and time variables, analytical solution is obtained in each separately layer in the Laplace domain before being numerically inverted in the original time domain. Analytical solution for this hypothetical scenario, based on the assumption of two input sources localized at the boundary was verified with using three tests cases of advection-dispersion problems with combination of two type of input boundaries. The accuracy of the methodology used is checked by comparing the results from the derived semi-analytical solutions the with those predicted by the previous analytical

methods as the GITT and those predicted by using numerical solution. Results show that for the four combination of input boundary, the multilayer analysis reproduces perfectly the solute distribution for the original transport problem in heterogeneous media. It accomplishes the validation of the mathematical formulations and analytical procedures obtaining the solutions. This approach is innovative and is all the more interesting because it can solve complex ADE without any difficulties. The prediction of the method to BOD demand show that the frequency of the sinusoidal input distribution considerably affects the solute distribution pattern. Our derived solution is quite general in that it can be applied to problems with variabe coefficient involving an arbitrary time-varying boundary conditions. The obtained solution can be used as a preliminary tool for analytical analyses and may helpful to predict the pollutant concentration distribution in the real case of two input contaminants sources. In future works, the methodology will be extended to one-dimensional multispecies transport problem with variables coefficients.

Appendix : Analytical Solution of the multilayer transport problem in the Laplace domain

In order to solve the multilayer transport model Eqs. (12)–(16), the model is reformulated into m isolated single-layer problems (Carr and Turner 2016; Rodrigo and Worthy 2016; Zimmerman et al. 2016, Carr 2020, Carr 2021). After, unknown functions of time, $g_i(t)(i = 1, ..., m-1)$ are introduce, to denote the following scalar multiple of the (negative) dispersive flux at the layer interfaces (Carr and Turner 2016; Rodrigo and Worthy 2016, Carr 2020, Carr 2021):

$$g_i(T) = \theta_i D_i \frac{\partial C_i}{\partial X}(l_i, T) \tag{A1}$$

yields Eqs. (12)-(16) for the multilayer transport to be written in the following equivalent model in each layer:

· First layer ($i = 1$)

$$R_1 \frac{\partial C_1}{\partial T} = D_1 \frac{\partial^2 C_1}{\partial X^2} - v_i \frac{\partial C_1}{\partial X} - k_1 C_1 + \gamma_1(T), \quad 0 \le X \le l_1 \tag{A2a}$$

$$C_1(X, T = 0) = f_1; \quad 0 < X < l_1 \tag{A2b}$$

$$a_0 C_1(X = 0, T) - b_0 \frac{\partial C_1(X = 0, T)}{\partial X} = g_0(T), \quad T \ge 0 \tag{A2c}$$

$$\theta_1 D_1 \frac{\partial C_1(X = l_1, t)}{\partial X} = g_1(T), \quad T \ge 0 \tag{A2d}$$

· Intermediary layer ($i = 1, ..., i = m-1$)

$$R_i \frac{\partial C_i}{\partial T} = D_i \frac{\partial^2 C_i}{\partial X^2} - v_i \frac{\partial C_i}{\partial X} - k_i C_i + \gamma_i(X), \quad l_i \le X \le l_{i-1} \tag{A3a}$$

$$C_i(X, T = 0) = f_i; \quad l_i < X < l_{i-1} \tag{A3b}$$

$$\theta_i D_i \frac{\partial C_i}{\partial X}(X = l_{i-1}, T) = g_{i-1}(T), \quad T \ge 0 \tag{A3c}$$

$$\theta_i D_i \frac{\partial C_i(X = l_i, T)}{\partial X} = g_i(T), \quad T \ge 0 \tag{A3d}$$

· Last layer ($i = m$)

$$R_m \frac{\partial C_m}{\partial T} = D_m \frac{\partial^2 C_m}{\partial X^2} - v_m \frac{\partial C_m}{\partial X} - k_m C_m + \gamma_m(T), \quad l_{m-1} \le X \le l_m \tag{A4a}$$

$$C_i(X, T = 0) = f_i; \quad l_i < X < l_{i-1} \tag{A4b}$$

$$\theta_m D_m \frac{\partial C_m}{\partial X}(X = l_{m-1}, T) = g_{i-1}(T), \quad T \ge 0 \tag{A4c}$$

$$a_L C(X = L, T) + b_L \frac{\partial C_m}{\partial X}(X = L, T) = g_L(T), \quad T \ge 0 \tag{A4d}$$

with each problem coupled together by imposing continuity of concentration at the interfaces between adjacent layers (Carr and Turner 2016; Rodrigo and Worthy 2016; Carr and March 2018, Carr 2020, Carr 2021).

Taking the Laplace transform of transport problem in each isolated single-layer Eqs. (A2a)-(A2d), (A3a)-(A3d), (A4a)-(A4d) yield:

$$D_1 \frac{d^2 \overline{C}_1}{dX^2} - v_i \frac{d\overline{C}_1}{dX} - (k_1 + sR_1)\overline{C}_1 + R_1 f_1 + \gamma_1(s), \quad 0 \le X \le l_1 \tag{A5a}$$

$$a_0 \overline{C}_1(X = 0, s) - b_0 \frac{d\overline{C}_1(X = 0, s)}{\partial X} = G_0(s) \tag{A5b}$$

$$\theta_1 D_1 \frac{d\overline{C}_1(X = l_1, s)}{dX} = G_1(s) \tag{A5c}$$

$$D_i \frac{d^2 \overline{C}_i}{dX^2} - v_i \frac{d\overline{C}_i}{dX} - (k + sR_i)_i \overline{C}_i + \overline{\gamma}_i(s) + R_i f_i, \quad l_i \le X \le l_{i-1} \tag{A6a}$$

$$\theta_i D_i \frac{d\overline{C}_i}{dX}(X = l_{i-1}, s) = G_{i-1}(s) \tag{A6b}$$

$$\theta_i D_i \frac{d\overline{C}_i(X = l_i, s)}{dX} = G_i(s) \tag{A6c}$$

$$D_m \frac{d^2 \overline{C}_m}{dX^2} - v_m \frac{d\overline{C}_m}{dX} - (k_m + sR_m)\overline{C}_m =$$
$$-\overline{\gamma}_m(s) - R_m f_i, \quad l_{m-1} \le X \le l_m \tag{A7a}$$

$$\theta_m D_m \frac{d\overline{C}_m}{dX}(X = l_{m-1}, s) = G_{i-1}(s) \qquad (A7b)$$

$$a_L \overline{C}_m(X = L, s) + b_L \frac{d\overline{C}_m}{dX}(L = L, s) = G_L(s) \qquad (A7c)$$

ACKNOWLEDGMENTS

GRANT SUPPORT DETAILS

CONFLICT OF INTEREST

The authors declare that there is not any conflict of interests regarding the publication of this manuscript.

LIFE SCIENCE REPORTING

No life science threat was practiced in this research.

REFERENCES

Al-Niami., A. N. S and Rushton K. R. (1979). Dispersion in stratified porous media. Water Resour. Res., 15 (5); 1044-1048.

Bharati, V. K., Singh, V. P., Sanskrityayn, A. and Kumar, N. (2017). Analytical solution of advection diffusion equation with spatially dependent dispersivity. J. Eng. Mech., 143(11); 1–11.

Bharati, V. K., Singh, V. P., Sanskrityayn, A. and Kumar, N. (2018). Analytical solutions for solute transport from varying pulse source along porous media flow with spatial dispersivity in fractal & Euclidean framework. Eur. J. Mech. B Fluids, 72; 410–421.

Bharati, V. K., Singh, V. P., Sanskrityayn, A. and Kumar, N. (2019). Analytical solution for solute transport from a pulse point source along a medium having concave/convex spatial dispersivity within fractal and Euclidean framework. J. Earth Syst. Sci., 128(203).

Carr, E. J., Turner, I. W. (2016). A semi-analytical solution for multilayer diffusion in a composite medium consisting of a large number of layers. Appl. Math. Model., 40; 7034-7050.

Carr, E. J. (2020). New semi-analytical solutions for advection-dispersion equations in multilayer porous media. Transp. Porous Med., 135; 39–58.

Carr, E. J. (2021). Generalized semi-analytical solution for coupled multispecies advection-dispersion equations in multilayer porous media. arXiv: 2006.15793v2 [Physics-Comp-Ph] 27 Jan 2021.

Chaudhary, M., Kumar, Thakur, C. and Singh, M. K. (2020). Analysis of 1-D pollutant transport in semi-infinite groundwater reservoir. Environmental Earth Sciences (2020) 79(24).

Chaudhary M. and Singh, M. K. (2020). Study of multispecies convection-dispersion transport equation with variable parameters. J. Hydrol. 591 (2020) 125562

Chen, J. S., Li, L. Y., Laia, K. H. and Liang, C. P. (2017). Analytical model for advective-dispersive transport involving flexible boundary inputs, initial distributions and zero-order productions.

S0022-1694(17)30587-5 DOI: http://dx.doi.org/10.1016/j.jhydrol.2017.08.050.

Das, P., Begam, S. and Singh, M. K. (2017). Mathematical modeling of groundwater contamination with varying velocity field. J. Hydrol. Hydromech., 65 (2); 192-204.

Djordjevich, A. and Savovic, S. (2013). Solute transport with longitudinal and transverse diffusion in temporally and spatially dependent flow from a pulse type source. Int. J. Heat and Mass Transfer, 65; 321-326.

Ema'a Ema'a, J. M., Ben-Bolie, G. H., Ele Abiama, P., Ali Zarma, Owono Ateba, P. (2015). A three-dimensional analytical solution for the study of air pollutant dispersion in a finite layer, Boundary-Layer Meteorol. DOI 10.1007/s10546-014-9997-0

Freeze, R. A. and Cherry, J. A. (1979). Groundwater, Prentice Hall, Englewood Cliffs, NJ.

Jaiswal, D. K., Kumar, A., Kumar, N., Singh, M. K. (2011). Solute transport along temporally and spatially dependent flows through horizontal semi-infinite media: dispersion proportional to square of velocity. J. Hydrol. Eng., 16 (3); 228-238.

Kumar, A., Jaiswal, D. K. and Kumar, N. (2010). Analytical solutions to one-dimensional advection–diffusion equation with variable coefficients in semi-infinite media. J. Hydrol., 380; 330-337.

Kumar, R., Chatterjee, A., Singh, M.K. and Singh, V.P. (2019). Study of solute dispersion with source/sink impact in semi-infinite porous medium. Pollution 6(1); 87-98.

Leij, F. J., Dane, J. H., and van Genuchten, M. Th. (1991). Mathematical analysis of one-dimensional solute transport in a layered soil profile. Soil Sci. Soc. Am., J. 55; 944–953.

Leij, F. J., van Genuchten, M. Th. (1995). Approximate analytical solutions for solute transport in two-layer porous media. Transp. Porous Med., 18; 65–85.

Liu, C., Ball, W. P., and Ellis, J. H. (1998). An analytical solution to the one-dimensional solute advection–dispersion equation in multi-layer porous media. Transp. Porous Med., 30; 25–43.

Liu, C., Szecsody, J. E., Zachara, J. M. and Ball, W. P. (2000). Use of the generalized integral transform method for solving equations of solute transport in porous media. Adv. Water Resour, 23; 483–492.

Manger, G. E. (1963). Porosity and bulk density of sedimentary rocks. U.S. Atomic Energy Commission USGPO, Washington, D.C.

Moreira, D. M., Tirabassi, T., Vilhena, M. T., and Goulart, A. G. (2010). A multi-layer model for pollutant dispersion with dry deposition to the ground. Atmospheric Environ. 44; 1859-1865.

Moreira, D. M., Vilhena, M. T., Tirabassi, T., Costa, C., and Bodmann, B. (2006. Simulation of pollutant dispersion in atmosphere by the Laplace transform: the ADMM approach. Water, Air and Soil Pollution, 177; 411–439.

Moreira, D. M., Vilhena, M. T., and Buske, D (2009). On the GILTT formulation for pollutant dispersion simulation in the atmospheric boundary layer. Air Pollution and Turbulence: Modeling and Applications, CRC Press, Boca Raton – Flórida (USA), 179–202.

Park, E. and Zhan, H. (2001). Analytical solution of contaminant transport from one-, two-, and three-dimensional sources in a finite-thickness aquifer. Journal of Contaminant Hydrology, 53; 41-61.

Pérez, Guerrero, J. S., Pimentel, L. C. G., Skaggs, T. H., and van Genuchten, M. Th. (2009). Analytical solution of the advection-diffusion transport equation using a change-of-variable and integral transform technique. Int. J. Heat Mass Transfer, 52(1314); 3297-3304.

Pérez, Guerrero, J. S., and Skaggs, T. H. (2010). Analytical solution for one-dimensional advection-dispersion transport equation with distance dependent coefficients. J. Hydrol., 390 (2010) 57–65.

Pérez Guerrero, J. S., Pimentel, L. C. G., and Skaggs, T. H. (2010). Analytical solution for the advection-dispersion transport equation in layered media. Int. Journal of Heat and mass transfert, 56(2013); 274-282.

Rodrigo, M. R., and Worthy, A. L. (2016). Solution of multilayer diffusion problems via the Laplace transform. J. Math. Anal. Appl. ,444; 475-502.

Rumer, R. R. (1962). Longitudinal dispersion in steady and unsteady flow. J Hydraul. Div. 88(HY4); 147-172.

Sanskrityayn, A., Bharati, V. K., and Kumar, N. (2016). Analytical solution of advection-dispersion equation with spatiotemporal dependence of dispersion coefficient and velocity using Green's function method. J. Groundwater Res. 5(1); 24-31.

Sanskrityayn, A., Bharati, V. K., and Kumar, N. (2018). Solute transport due to spatio-temporally dependent dispersion coefficient and velocity: analytical solutions. J. Hydrologic Engineering, 23(4); 04018009.

Scheidegger, A. E. (19957). The physics of flow through porous media. University of Toronto Press,

Toronto.

Serrano, S. E. (1992). The form of the dispersion equation under recharge and variable velocity, and its analytical solution. Water Resour. Res., 28(7); 1801-1808.

Sim, Y. and Chrysikopoulos, C.V. (1996). One-dimensional virus transport in porous media with time-dependent inactivation rate coefficients. Water Resour. Res. 32(8); 2607–2611.

Singh, M. K. and Das, P. (2015). Scale dependent solute dispersion with linear isotherm in heterogeneous medium. J. Hydrol., 520; 289–299.

Singh, M. K. and Kumari, P. (2014). Contaminant concentration prediction along unsteady groundwater flow. In: Basu SK, Kumar N (eds) Modelling and simulation of diffusive processes. Springer, Cham, 257–275.

Thakur, C. K., Chaudhary, M., van der Zee, S. E. A. T. M. and Singh, M. K. (2019). Two-Dimensional solute transport with exponential initial concentration distribution and varying flow velocity. Pollution, 5(4); 721-737, Autumn 2019.

Trefethen, L. N., Weideman, J. A. C., Schmelzer, T. (2006). Talbot quadratures and rational approximations. BIT Numer. Math., 46, 653–670.

Yadav, R. R., Kumar, L. K. (2018). Two-dimensional conservative solute transport with temporal and scale-dependent dispersion: analytical solution. International Journal of Advance in Mathematics, 2018 (2), 90-111.

Zimmerman, R. A., Jankowski, T. A., Tartakovsky, D. M. (2016). Analytical models of axisymmetric reaction-diffusion phenomena in composite media. Int. J. Heat Mass Tran., 99, 425-431.